

Development of a 4kx4k frame transfer electron multiplying CCD for scientific applications

Jean-Luc Gach^{1,a}, Claude Carignan^{b,c}, Olivier Hernandez^{c,d}, Paul R. Jordan^e, Douglas Jordan^e,
Philippe Balard^a, Philippe Vallée^c, Philippe Amram^a, Michel Marcelin^a, Benoit Epinat^a

^aAix Marseille Université, CNRS, LAM (Laboratoire d'Astrophysique de Marseille) UMR 7326,
13388 Marseille, France;

^bUniversity of Cape Town, Department of Astronomy, Rondebosch 7701, South Africa;

^cUniversité de Montréal, Département de Physique, CRAQ, Montréal H3C 3J7, Québec, Canada;

^dObservatoire du Mont Mégantic, Notre dame des Bois J0B 2E0, Québec, Canada;

^eE2V technologies, 106 Waterhouse Lane, Chelmsford, Essex, CM1 2QU, England;

ABSTRACT

The CCD282 is a large low-light level (L3 - Electron multiplying CCD) imaging sensor developed by e2v technologies for the University of Montreal. The intended use is for photon counting and very low light level imaging. The device will be used on the 3DNTT instrument which is a scanning Fabry-Perot interferometer. There is also the intention to place a device on a 10m class telescope for scanning Fabry-Perot application. This sensor is the largest electron multiplying CCD device produced to date with a 4kx4k backside illuminated frame transfer architecture. The sensor uses 8 parallel EM (Electron Multiplying) amplified outputs to maximize throughput. This paper presents the first results and performance measurements of this device, and especially of the clock induced charge (CIC) which is one order of magnitude lower than previous devices thanks to a specific design optimized for photon counting operation.

Keywords: EMCCD, Electron Multiplying CCD, L3Vision CCD, L3CCD, photon counting, low readout noise.

1. INTRODUCTION

Since Electron Multiplying CCDs (EMCCDs) appeared in 2001 [1], they've showed their ability to make images of extremely faint flux scenes for many various scientific applications like astronomy, life sciences, physics or general purpose applications like night vision. The first devices were rather small (TV format), but larger (up to 1kx1k) back thinned devices optimized for scientific applications were developed by E2V in the 2000's (CCD97, CCD201). Special devices optimized for wavefront sensing showed the ability of this technology to deal with fast frame readout applications and to now the CCD220 is still the fastest low noise scientific EMCCD exhibiting more than 150 Mpixels/s throughput while maintaining a sub electron readout noise. This device was also the first EMCCD to use deep depletion silicon and to have an integral shutter version (CCD 219 [3]). But to date no large format EMCCD devices were produced in large format compatible with the use of a focal plane instrument of a 10-m class telescope. This is mainly due to the fact that wide field observations are usually photon noise limited, and the use of an EMCCD won't increase the SNR of the observations. But for some photon starved applications (narrow band imaging, high spectral resolution spectroscopy or spectro-imagery) or time resolved applications (high spatial resolution imaging), the use of an EMCCD would increase the SNR. This is particularly the case with Fabry-Perot 3D-imaging where the spectral resolution of an elementary image may lead to only a few photons per pixel and per hour of signal when observing extragalactic faint objects like low surface brightness galaxies. Also for this kind of scanning instruments, the time resolution is a key parameter to smooth the atmosphere transmission and sky lines variations, and the experience showed that a full scan (20 to 100 channels) must be done in no more than 20 minutes to ensure an acceptable photometric stability, leading to

¹ Jean-luc.gach@lam.fr ; phone +33 (0)4 95044119 ; fax +33 (0)4 91621190

elementary exposures in the range of 10 seconds. The whole observation is done by summing up several see-saw scanning averaging the sky variations. An elementary exposure of 10s at a spectral resolution of 5000 to 20 000 will have only a few photons, making sense to use an EMCCD in photon counting mode.

2. THE CCD282

The CCD282 is a split frame transfer 4112x4096 pixels image sensor (see Figure 1). Each half-image section will output on 4 separate serial and EM gain registers providing 8 parallel outputs. This device takes the benefit from the CCD220 multiple output EM development, optimizing throughput and frame rate for time resolved applications.

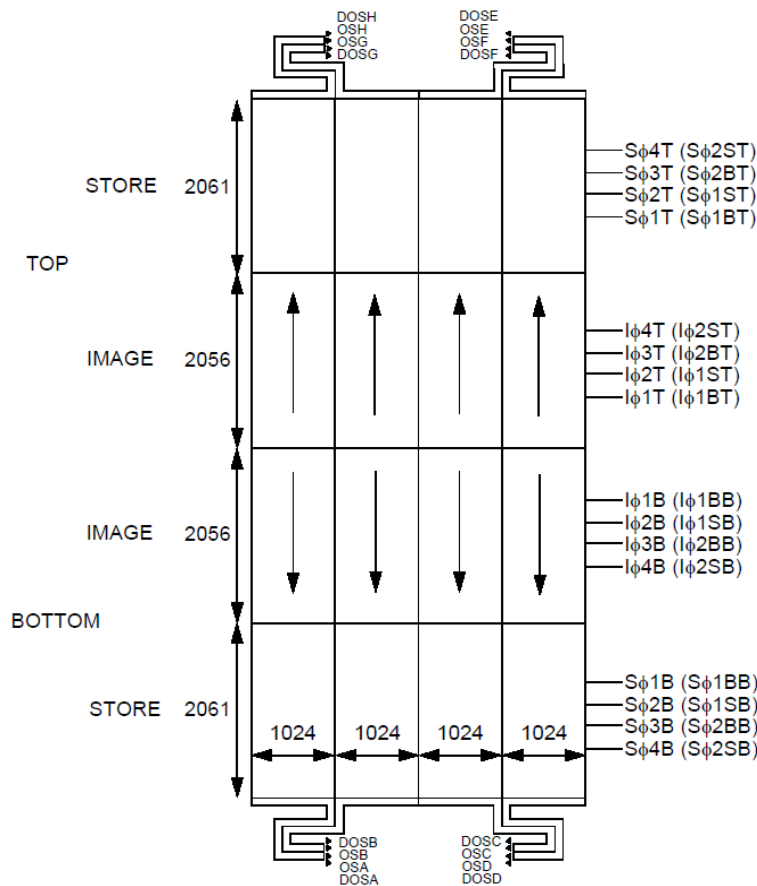


Figure 1: The CCD282 8 output split frame transfer architecture.

Each output is designed for a 15MHz readout and the frame rate is limited by the R-C time constant formed by the parallel clock polysilicon connection and the pixel capacitance, leading to a 6 μ s line transfer time and a frame rate greater than 5 frames per second. The device is back thinned and glued to a multilayer aluminium nitride pin grid array package (see Figure 2). The package includes two temperature sensors to measure accurately the CCD temperature. Both the top surface and the bottom surface of the package are ground, to ensure good flatness, required to achieve an image area flatness of better than 20 μ m and a good thermal interface to the bottom of the package. Areas to either side of the CCD are provided to allow space to clamp the package to a thermal interface (cold finger) to provide good thermal contact. The whole device has been optimized for photon counting applications, focusing on the throughput and clock induced charge (CIC) minimization.

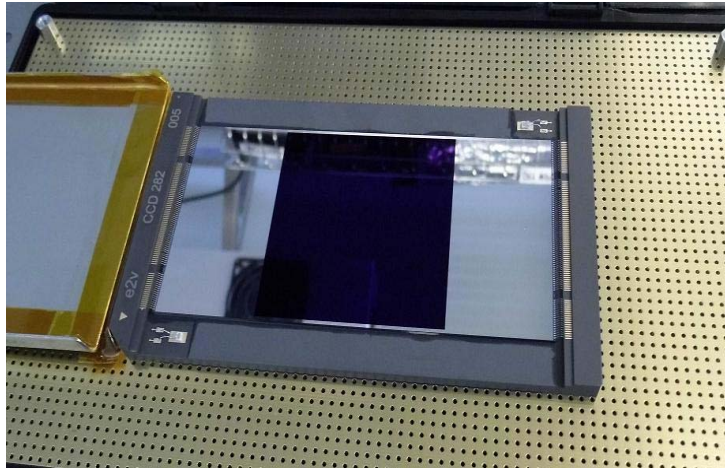


Figure 2: A view of the packaged CCD282 in its aluminium nitride multilayer pin grid array package © E2V.

3. CLOCK INDUCED CHARGE MINIMIZATION

The clock induced charge phenomenon has been raised as soon as people were interested in EMCCD for photon counting applications as a potential replacement of intensified photon counting systems [4]. The clock induced charge is a parasitic electron generated while the CCD is read-out. For each charge transfer, there is a probability that the moving electrons (or holes in N-type silicon) generate a secondary electron by impact ionization. The same phenomenon is used for charge multiplication in EM gain registers. This phenomenon was known before EMCCDs as spurious charge, and was lowered to invisible levels in standard CCDs, but as soon as EMCCDs have a subelectron readout noise, this becomes visible again. Of course this parasitic events act as noise in photon counting applications and need to be minimized. There are several parameters to minimize clock induced charge. First of all, it is preferable to use the device in non-inverted mode operation (NIMO) because inverted mode (IMO) generates more CIC. This is because when the device is in NIMO mode, holes appear in the N-type silicon surrounding the P-well. These holes will recombine surface dark current electrons preventing them to reach the collecting P-well. But when clocking the device, the moving holes (to the channel stop) will generate more CIC than a device running in non-inversion. To compensate for the extra dark current in the device, it is then necessary to cool it deeper (-110°C typically). The second most important parameter for CIC is clock amplitude. As for EM gain, the CIC will raise exponentially with clock voltage (see [6]). Lower clock amplitude will then minimize CIC. But for parallel clocks, there is a minimal voltage where the transfer won't occur anymore. This is due to the well barrier implant, creating a static field in the silicon, field that is necessary to overcome to have a good charge transfer (see Figure 3).

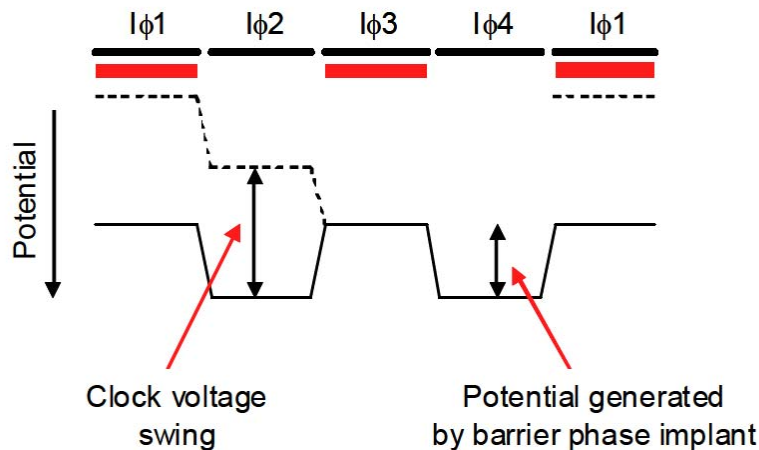


Figure 3 : Potential across a 2-phase device. The clocking must overcome the static electric field generated by the barrier implant to have charge transfer (dashed line).

Hence, the strategy was to lower the barrier implant dose to minimize the clock amplitude. This barrier implant determines also the full well capacity (FWC) of the CCD device, but for photon counting applications, it is clear that FWC is a minor concern. A reasonable tradeoff has been proposed by E2V during the device simulation phase, and the targeted FWC is 50 000 electrons. It is believed that other parameters have only a secondary effect on the CIC. In that sense, the wave shaping used in [5] never had any reasonable explanation up to now. One explanation given was the slower electron mobility due to the slower phase rise time. But even with rise times in the order of magnitude of 1ns, the electron speed is still 5000 times lower than the necessary energy to reach the threshold energy to have impact ionization. Maes et al. [6] and many other authors before him showed that the relevant parameter for impact ionization is the local electric field. Therefore we interpret the effect of minimization of CIC by wave shaping simply by the way to optimize charge transfer while maintaining the clock amplitude near the minimal possible level (especially due to the R-C network seen on the driver side). It is also a way to minimize the clock overshoots that raise the electric field under the clock electrode. Wave shaping has probably no direct impact on CIC. We'll see later on that with a standard clocking, the gain with this implant optimization and clock amplitude minimization gives far better results.

The CIC phenomenon is a probabilistic event that has a chance to occur on each transfer, therefore it is directly proportional to the number of transfers occurring in the device. In that sense large devices are more subject to CIC than smaller ones. By using a split frame transfer with 8 outputs, the number of transfers is kept to a reasonable level.

4. CCD 282 MEASURED PERFORMANCE

4.1. Imaging performance

The CCD282 ability of producing images was a concern because of the implant dose reduction. Figure 4 shows the first images obtained by E2V at -60°C with a 2MHz controller readout. This image shows clearly the bias and gain discrepancy of each of the eight image section. However the gain of each amplifier has been measured by E2V with a Fe55 source and shows that all the amplifiers are well matched with a +/-2% gain deviation.

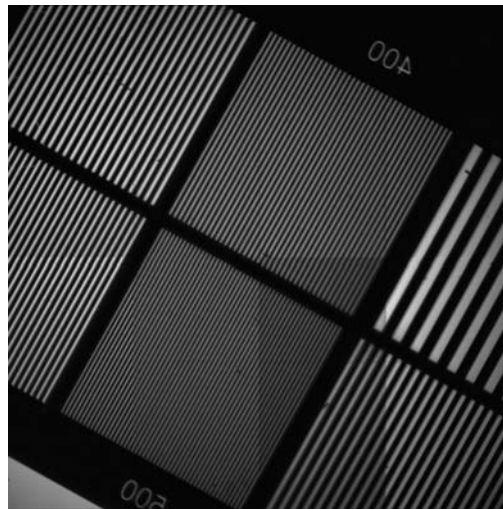


Figure 4 : The CD282 first image taken at -60°C

4.2. Clock induced charge

The clock induced charge was measured separately for the parallel CIC (generated by parallel transfers) and serial CIC. For the first one, 1 000 000 rows were binned in the serial register (each having 4112 transfers) and each resulting line was corrected from the average dark signal at different parallel clock voltages. The graph in Figure 5 shows the clear dependence of the clock amplitude with the generated CIC. With this device, as it is possible to lower the parallel clock

voltage to very low levels, the parallel clock CIC lowers to nearly non measurable levels, below 10 CIC events per frame which is a major breakthrough.

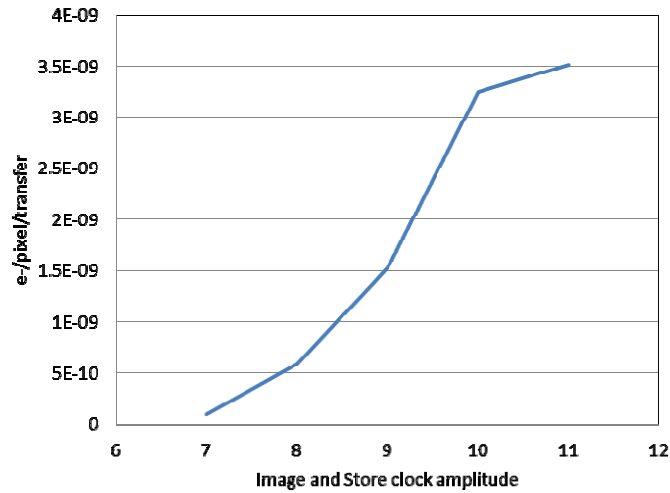


Figure 5 : Generated parallel CIC VS clock amplitude in volts

The serial clock induced charge is measured using the overscan regions. As for the parallel register the dependence of the CIC level vs clock amplitude is also demonstrated here, but for serial clocking, there is no barrier implant therefore the only limit is the CTE achieved due to the DC electrode and the phase amplitude which is at a constant level. The HV clock amplitude (gain) is also a second order parameter. The graph in Figure 6 shows this double dependence, and with the current parameters a minimum of 0.06% of CIC for 2080 transfers is obtained resulting in 3.10^{-7} e-/pixel/transfer of CIC.

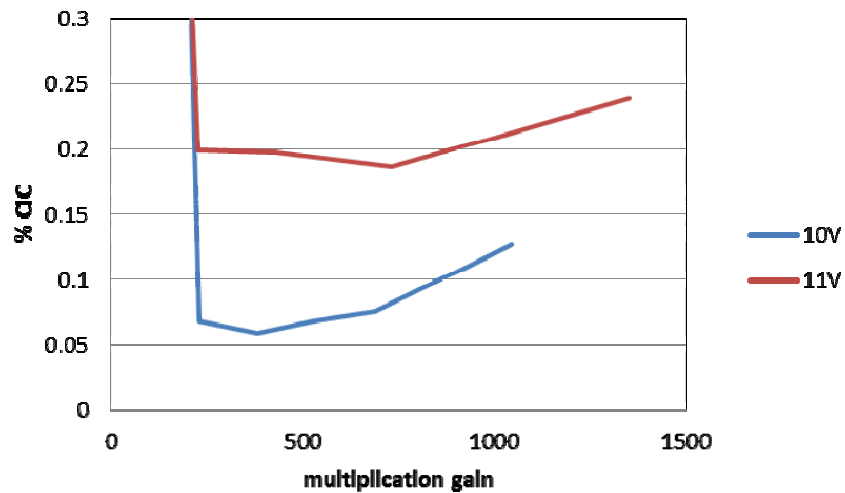


Figure 6 : serial CIC level vs multiplication gain and serial clock amplitude

Clearly the CIC level is dominated by serial transfer in this device, but further investigations and serial clock amplitude minimization will be carried out to lower further the CIC.

Considering an operation at -110°C and a 5FPS frame rate, the total spurious charge comes to 10 e^{-} from the parallel CIC, 1000 e^{-} from the dark current and $10\ 000\text{ e}^{-}$ from the serial CIC, totalizing $\sim 11\ 000$ electrons, equivalent to $0.0006\text{ e}^{-}/\text{pix}/\text{frame}$ which is the lowest spurious level ever obtained. This extremely low level has been obtained in spite of the

large format of the CCD which is not in favor of this, compared to smaller devices like the CCD97 or CCD201. If we scale the spurious events of the CCD282 to the size of these smaller devices, this equals to more than one order of magnitude less spurious events than the previous generation of EMCCDs.

5. APPLICATIONS

As explained above, the design of the device was optimized for photon counting applications. As shown in [7], this is in that regime and in fast read-out applications (low fluxes with e.g. astronomical flux densities $< 10^{-16}$ Erg/s/cm²/arcsec² [8]) that EMCCDs really gain a lot over conventional CCDs. This is why, at the moment, the first applications for the new chips are for 3 scanning Fabry-Perot systems: the 3DNTT on the 4m NTT telescope in Chile, the scanning Fabry-Perot on the 1m MARLY telescope in Burkina Faso and hopefully (discussions are underway) on the OSIRIS Fabry-Perot system on the GranTeCan 10m telescope. Other applications are being explored for the 3 more chips that will be produced in the first batch.

5.1. 3DNTT

The 3D-NTT is a seeing limited visible integral field spectro-imager to be attached at the Nasmyth focus of the NTT [9]. Basically it is a focal reducer inside which Fabry-Perot interferometers of low or high interference order can be placed separately or simultaneously, offering different observing modes (low or high resolution). The niche for 3D-NTT is extended object or/and large filling factor, emission lines and versatile spectral resolution.

Thanks to its ability to work at low or high resolution, the 3D-NTT can be used for a large variety of scientific programmes. However, it will mainly focus on two large programmes: *"Characterizing the interstellar medium of nearby galaxies"* and *"Gas accretion and radiative feedback in the early universe"*.

This instrument is being built as a collaborative effort between LAM (Marseille), GEPI (Paris), LAE (Montréal) and IAG (Universidade de São Paulo, Brazil).

Two different detectors were originally envisioned for the two modes of this instrument [9] but the CCD282, because of its high performances, will be the detector used for both low and high resolution modes of this instrument.

The low resolution mode will provide a large field of view (17 arcmin x 17 arcmin) covering the whole surface of the CCD and the high sensitivity of the CCD282 in the blue will allow reaching the [OII] line at 372.7 nm which is of peculiar interest for metallicity measurements in galaxies.

The high resolution mode will provide a smaller field of view (circular, 9 arcmin diameter). This mode will be mainly used for scanning emission lines of galaxies or nebulae, in order to get their detailed profile and measure their radial velocity. Such a scan is obtained through series of short exposures made with different values of spacing between the plates of the Fabry-Perot interferometer, necessitating a specific detector. The CCD282 is well adapted to this task since it is able to operate in photon counting mode, thanks to its very low spurious charges generation rate and sub-electron (< 0.1 electron) effective readout noise. This enables to scan rapidly the interferometer (typically 5 to 10 s exposure time for a given spacing of the plates) and to average out the changes in transparency due to weather conditions or airmass variations along the exposure.

6. CONCLUSION

The CCD282 is the largest EMCCD ever built with 4kx4k active pixels. It has been optimized for photon counting applications and shows the lowest spurious charge (dark + CIC) ever achieved by an EMCCD device, ten times lower compared to the other devices. This has been obtained with a classical controller device, not particularly tuned to obtain the best results and further optimization, especially with serial register, will lower even further the spurious charge generated by the device.

REFERENCES

- [1] P. Jerram, P. J. Pool, R. Bell, D. J. Burt, S. Bowring, S. Spencer, M. Hazelwood, I. Moody, N. Catlett, and P. S. Heyes, "The LLCCD: low-light imaging without the need for an intensifier", in Proc. SPIE, 4306, pp. 178-186, May 2001.
- [2] P. Feautrier, J.L. Gach, P. Balard, C. Guillaume, M. Downing, N. Hubin, E. Stadler, Y. Magnard, M. Skegg, M. Robbins, S. Denney, W. Suske, P. Jordan, P. Wheeler, P. Pool, R. Bell, D. Burt, I. Davies, J. Reyes, M. Meyer, D. Baade, M. Kasper, R. Arsenault, T. Fusco, J. Javier Diaz-Garcia, "Characterization of OCam and CCD220: the fastest and most sensitive camera to date for AO wavefront sensing", in Proc. SPIE, 7736, June 2010.
- [3] J.L. Gach, P. Feautrier, P. Balard, C. Guillaume, E. Stadler "OCAM2S: an integral shutter ultrafast and low noise wavefront sensor camera for laser guide stars adaptive optics systems", in Proc. SPIE, 9148, June 2014.
- [4] J.L. Gach, C. Guillaume, O. Boissin, C. Cavadore "First results of an L3CCD in photon counting mode", ASSL 300, p611, 2004.
- [5] O. Daigle, J.L. Gach, C. Guillaume, S. Lessard., C. Claude, S. Blais-Ouellette "CCCP : a CCD controller for counting photons", in Proc. SPIE, 7014, August 2008.
- [6] W. Maes, K. De Meyer, R. Van Overstraeten, "Impact ionization in silicon: a review and update" Solid State Electronics 33, n°6 pp 705-718, 1990.
- [7] Gach, J.-L., Hernandez, O., Boulesteix, J., Amram, P., Boissin, O., Carignan, C., Garrido, O., Marcelin, M., Östlin, G., Plana, H., Ra.pazzo, R. "Fabry-Perot Observations Using a New GaAs Photon-counting System", PASP, 114, 1043, 2002.
- [8] Hernandez, O., Fathi, K., Carignan, C., Beckman, J., Gach, J.-L., Balard, P., Amram, P., Boulesteix, J. Coradi, R. L. M., de Denus-Baillargeon, M.-M., Epinat, B., Relano, M., Thibault, S., Vallée, P. GHaFaS: "Galaxy H-alpha Fabry-Perot System for the WHT", Publications of the Astronomical Society of the Pacific, 120, 665, 2008
- [9] M. Marcelin, P. Amram, P. Balard, C. Balkowski, O. Boissin, J. Boulesteix, C. Carignan, O. Daigle, M-M. de Denus Baillargeon, B. Epinat, J-L. Gach, O. Hernandez, F. Rigaud, and P. Vallée, "3D-NTT: a versatile integral field spectro-imager for the NTT", in Proc. SPIE, Volume 7014, pp. 701455-701455-8